

**Methanol Droplet Extinction in Oxygen/Carbon-dioxide/Nitrogen Mixtures in Microgravity:  
Results from the International Space Station Experiments**

V. Nayagam<sup>1</sup>, D. Dietrich<sup>2</sup>, P. Ferkul<sup>1</sup>, M. C. Hicks<sup>2</sup> and F. A. Williams<sup>3</sup>

<sup>1</sup>National Center for Space Exploration Research, Cleveland, Ohio

<sup>2</sup>NASA Glenn Research Center, Cleveland, Ohio

<sup>3</sup>Department of Mechanical and Aerospace Engineering, UCSD, La Jolla, CA

**Abstract**

Motivated by the need to understand the flammability limits of condensed-phase fuels in microgravity, isolated single droplet combustion experiments were carried out in the Combustion Integrated Rack facility onboard the International Space Station. Experimental observations of methanol droplet combustion and extinction in oxygen/carbon-dioxide/nitrogen mixtures at 0.7 and 1 atmospheric pressure in quiescent microgravity environment are reported for initial droplet diameters varying between 2 mm to 4 mm in this study. The ambient oxygen concentration was systematically lowered from test to test so as to approach the limiting oxygen index (LOI) at fixed ambient pressure. At one atmosphere pressure, ignition and some burning were observed for an oxygen concentration of 13% with the rest being nitrogen. In addition, measured droplet burning rates, flame stand-off ratios, and extinction diameters are presented for varying concentrations of oxygen and diluents. Simplified theoretical models are presented to explain the observed variations in extinction diameter and flame stand-off ratios.

**Introduction**

Combustion of isolated, single droplets in a microgravity environment has provided valuable insights into the fundamental burning characteristics of liquid fuels in the past. The FLEX experiments, currently underway in the International Space Station (ISS), exploit the microgravity droplet combustion process to investigate the fire safety aspects of space exploration environments. Methanol and heptane fuel droplets are burned in carbon dioxide and nitrogen diluted environments with varying amounts of oxygen, and pressures. Here we present the results for methanol droplet experiments that were recently completed.

**Experiments**

The experiments were conducted using the Multi-User Droplet Combustion Apparatus (MDCA) installed in the Combustion Integrated Rack (CIR) facility in the US Module of the ISS. The cylindrical combustion chamber in the CIR has a free-volume of approximately 95 liters with the MDCA insert installed. The MDCA used an opposed-needle deployment technique to freely deploy droplets of chosen size in microgravity. Ignition of the free-floated droplet was accomplished using two symmetrically positioned hot-wire igniters. The experimental diagnostic system consisted of a black-and-white, back-lit droplet image capture camera, a UV-sensitive flame imaging camera filtered to observe OH\*-chemiluminescence at 310 nanometer wave length, and a CCD color camera with a wider view angle. All the camera images are digitally stored on-board the CIR and down-linked at a later time for analysis. The color camera with its real-time

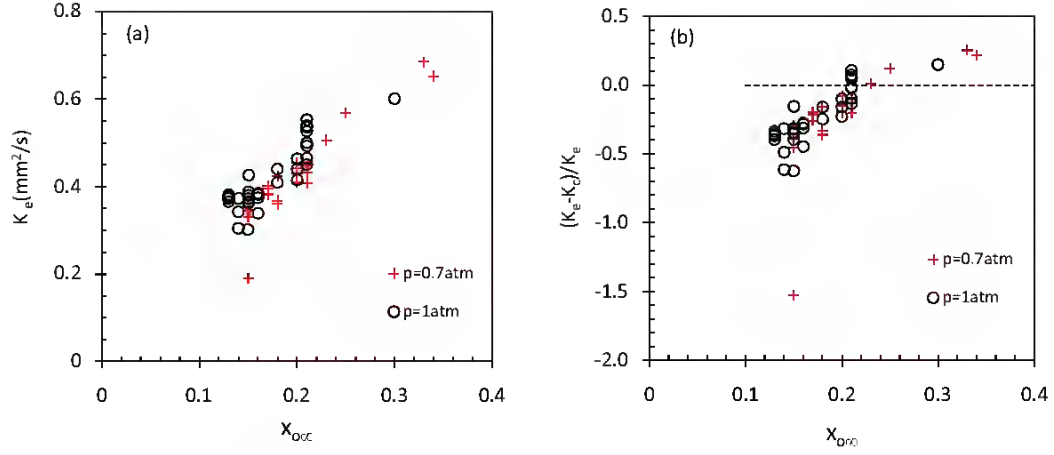


Figure 1: (a) Measured burning rate constant versus ambient oxygen mole fraction; (b)  $(K_e - K_c)/K_e$  as a function of ambient oxygen mole fraction.

down-link capability is also used to conduct experiment operations from the ground at the Tele-science Support Center located in NASA Glenn Research Center. Prior to an experimental run, the Fuel and Oxidizer Management Assembly (FOMA) system of the CIR is used to fill the combustion chamber with the desired ambient gas mixture consisting of oxygen, nitrogen, and carbon dioxide at a selected pressure. Typically several droplet burns were performed in each environment before venting the combustion chamber to space vacuum and refilling. Further details of experiments and operational procedures can be found in Dietrich et al [1].

## Results and Discussion

Over two hundred droplet burns were carried out using methanol and heptane fuels in varying ambient gas mixtures containing oxygen/nitrogen/carbon dioxide with initial droplet diameters in the range of 2 to 4 mm at the time this report was prepared. Out of these, there were 104 methanol tests of which 54 tests yielded extinction diameters where the droplet remained in the field of view of the hack-lit camera. Results of these 54 methanol tests are examined in this study.

### Average Burning Rates

Droplet diameters as a function of time were obtained from the digital images of the droplet-view camera. The burning rate constant  $K_e$  is obtained from the slope of the  $d^2$  versus time plots. Figure 1a shows  $K_e$  as a function of ambient oxygen mole fraction  $x_{O_2}$ . The burning rate decreases with decreasing oxygen concentration, as one would expect. For a fixed oxygen concentration, increasing  $CO_2$  levels at the expense of  $N_2$  tends to slightly decrease the  $K$  values. The measured  $K_e$  values can be compared against classical quasi-steady theoretical values  $K_c$ . The fractional deviations from the quasi-steady values, i.e.  $(K_e - K_c)/K_e$ , as a function of  $x_{O_2}$  are shown in Fig 1b. Clearly at low oxygen concentrations the burning rate constant deviates substantially from the quasi-steady predictions.

### Flame Stand-off Ratio

The flame stand-off ratio ( $d_f/d$ ) was calculated as a function of time from the measured droplet diameter  $d$ , and flame diameter  $d_f$ . Flame diameters were obtained from both the UV and the CCD-camera images using frame-by-frame analysis. Typically, during an experimental run the flame stand-off ratio remains approximately at a constant value away from the initial ignition

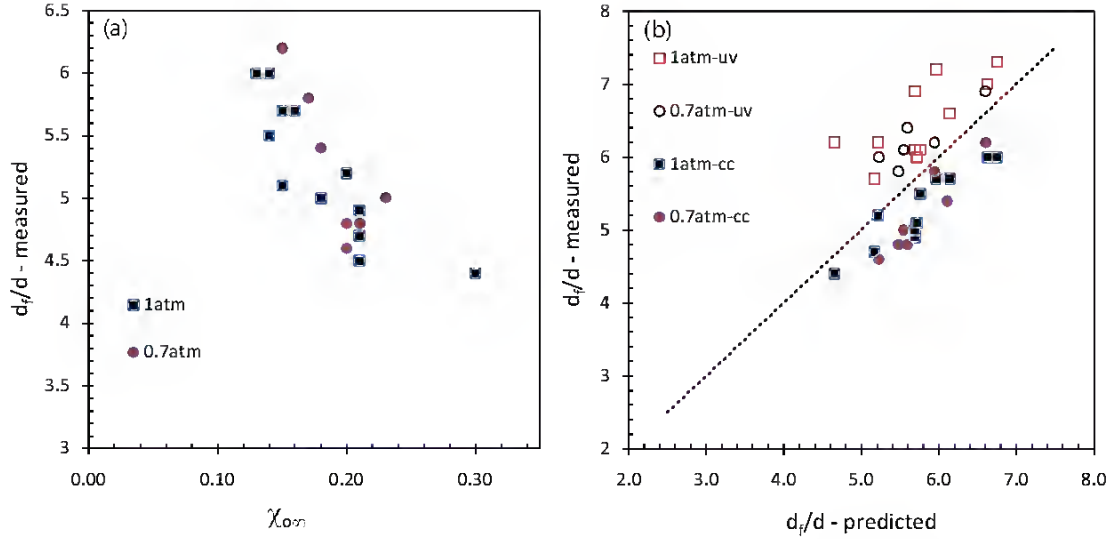


Figure 2: (a) Flame stand-off ratio vs ambient oxygen mole fraction; (b) Measured vs predicted flame stand-off ratio.

and final extinction periods. Figure 2a shows the variation of average flame stand-off ratio as a function of ambient oxygen mole fraction  $x_{O_2}$  for both 0.7 atm and 1 atm, with each data point representing a unique ambient condition. The average values were obtained during the quasi-steady time period when the stand-off ratio remains approximately constant. As one would expect,  $d_f/d$  increases with decreasing ambient oxygen mole fraction since the flame needs to move farther away to meet the stoichiometric requirement.

It is also possible to correlate the measured flame stand-off ratio against a simplified, quasi-steady theoretical model that includes the effects of water absorption, developed by Nayagam [2]. This model uses the measured burning rate constant  $K$  and the calculated effective oxygen and water vapor diffusion coefficients  $D_o$  and  $D_w$  and predicts the flame stand-off ratio to be

$$\frac{d_f}{d} \approx \frac{1}{2} \left[ a + \sqrt{a^2 - 2a + 4b + 1} + 1 \right], \quad (1)$$

where,  $a = \left( \frac{W_{av}\nu_o\rho_f K}{8W_f\nu_f\rho_g D_o} \right) \frac{1}{x_{O_2}}$ , and  $b = \frac{W_w\rho_f}{W_f\rho_w} \frac{\nu_o D_w x_{w,f}}{\nu_f D_o x_{O_2}}$ . Here  $W$ ,  $\nu$ ,  $\rho$ , and  $D$  are the molecular weight, stoichiometric coefficient, density and effective diffusivity respectively, and the subscripts,  $f$ ,  $w$ ,  $g$ ,  $av$ , and  $\infty$  refer to fuel, water vapor, gas, average gas-phase, and ambient respectively. Figure 2b shows the measured flame stand-off ratios plotted against the predicted values using Eq. (1). The UV data report the outermost digitally enhanced threshold of detected intensity and thus correspond to the outer boundary of the reaction zone, while the CC data correspond to peak visible-range intensity which may have contributions from fuel molecules, possibly biasing it toward smaller diameters. Overall, the results therefore appear to compare well with predictions. It is also interesting to note that Eq. (1) shows close agreement with experimental values even at low oxygen concentrations since the measured burning rate constants are used rather than the quasi-steady theoretical values.

### Extinction Diameter

Figure 3 shows the droplet extinction diameter as a function of the initial diameter for experiments at 1 atm with the oxygen content of the atmosphere ranging from 13% to 21%. The inert

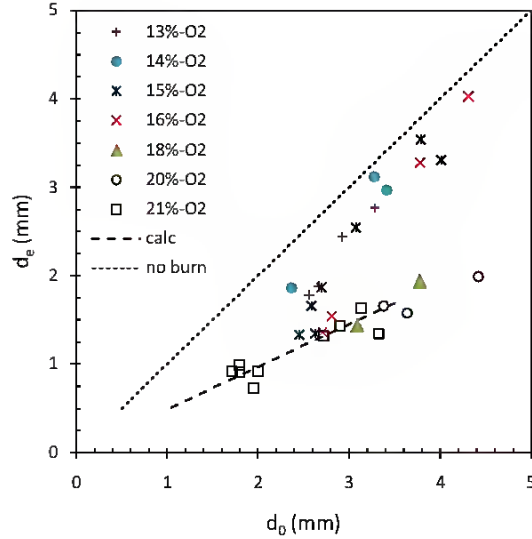


Figure 3: Extinction diameter as function of initial diameter at 1 atm pressure.

gas was pure nitrogen or mixtures of nitrogen and carbon dioxide. In most mixtures there was more  $N_2$  than  $CO_2$ , but one of the tests at 21%  $O_2$  had 70%  $CO_2$  and 9%  $N_2$ .

The data are seen to fall roughly into two bands. The extinction diameters are small for  $O_2$  concentrations of 18 % or above but near the initial diameter (the no-burn line) for  $O_2$  concentrations of 14 % or below. The points at 15 % and 16 %  $O_2$  migrate from the small-extinction-diameter group to the large-extinction-diameter group with increasing initial diameter, departing from the small-diameter range later, at a larger initial diameter, for the higher  $O_2$  concentration. This behavior is entirely consistent with transition from diffusive to radiative extinction. The upper group exhibits radiative extinction and the lower group diffusive extinction. In 18 % or more  $O_2$  all droplets exhibit diffusive extinction, and in 14 % or less  $O_2$  all exhibit radiative extinction, there being critical initial diameters separating the two limiting behaviors at the two intermediate  $O_2$  concentrations. The points at 14 %  $O_2$  that lie closer to the no-burn line than those at 13 %  $O_2$  had more  $CO_2$  in the atmosphere, suggesting that this diluent promotes radiative extinction, as expected from its much greater infrared emissivity. On the other hand, one of the three diffusive-extinction points at the smallest initial diameters had 70 %  $CO_2$ , indicating that the influence of this inert on diffusive extinction is not very different from that of  $N_2$ .

To complement full numerical computations and to provide a different perspective for understanding, the theory of Zhang et al. [3] was applied to this data. That theory considers quasi-steady, spherically symmetrical burning, accounting for water absorption in the droplet. The limits of liquid-phase water diffusion through methanol and of a well-mixed liquid were both addressed. The latter is the realistic one as a consequence of strong solutal-Marangoni (diffuso-capillary) instability, and it is the limit considered here. Gas-phase Lewis numbers are taken to be unity since that was shown [4] to be a sufficiently accurate approximation. From solutions of gas-phase conservation equations for fuel and water concentrations and for temperature in the flame-sheet limit of infinite reaction rates, a pair of nonlinear ordinary differential equations eventually was derived for the dependence of the liquid temperature and the water concentration in the liquid on the droplet diameter. In the present work, this pair of equations was integrated

numerically for the specific atmospheres of the present experiments.

Zhang et al.[3] also applied rate-ratio asymptotics for effects of finite-rate chemistry to calculate extinction diameters of droplets. Plots of droplet diameters and extinction diameters as functions of time then determined extinction conditions from the time at which these two diameters became equal. Results of rate-ratio asymptotics, as well as of detailed chemical-kinetic calculations, often predict extinction to occur at a more or less fixed flame temperature, somewhere between about 1300 K and 1600 K, depending on the atmosphere and on conditions. For this reason, in the present work, extinction conditions are considered instead in terms of flame temperatures. Actual flame temperatures at extinction are most relevant, and they are a few hundred degrees below infinite-rate adiabatic flame temperatures. As a rough indication of what those temperatures might be, however, the experimental extinction diameters will be compared with droplet diameters calculated for fixed values of those infinite-rate, adiabatic temperatures.

As the droplet begins to burn, some of the water produced in the flame diffused back to the surface of the droplet and is absorbed in the liquid. The water concentration in the liquid then gradually builds up during time. During this phase of burning, the flame temperature remains practically constant. Eventually the water content of the liquid increases to a point at which water begins to vaporize along with the fuel, and the water flux in the gas changes direction. The mixture vaporizing and flowing to the flame then becomes increasingly dilute, correspondingly reducing the flame temperature. In air, for example, the calculated infinite-rate flame temperature of 1815 K then is calculated to decrease to 1300 K in a period of time during which the droplet diameter decreases by about a factor of two. The initial decrease after the zero-water-flux condition is noticeably steep, and so the true flame extinction temperature may be expected to be reached shortly after the zero-flux condition. The calculated zero-flux condition for air does, in fact, provide a tight upper bound for the lower group of points in Figure 3. The line shown in the figure, marked calculation, corresponds to a calculated infinite-rate flame temperature of 1800 K. A correspondingly calculated line of 1750 K provides a tight lower bound for the lower group. It may thus be concluded that diffusive extinction occurs when the infinite-rate ideal flame temperature decreases to a value not far from 1800 K in atmospheres having  $O_2$  contents of 21 %. That value decreases with dilution and is less than 1650 K at 18%.

Since the calculations discussed above all neglect radiant energy loss, they cannot address radiant extinction. The calculations can be revised to include radiant energy loss by artificially decreasing the value of the heat release per unit mass of oxidizer consumed to provide an effective net heat release. To estimate the extent of decrease the ratio of the rate of radiant energy loss to the rate of heat release must be estimated, which involves estimating Planck-mean absorption lengths for  $H_2O$  and  $CO_2$  in the flame. If such an estimate is made for one droplet size, however, then the effective net heat release can be estimated for any droplet size by observing that the rate of heat release is proportional to the product of the surface area and the gradient, while the rate of radiant loss is proportional to the product of the surface area and the flame thickness. The former thus is proportional to the droplet diameter, and the latter to the cube of the droplet diameter, so that the ratio varies as the square of the diameter. The radiant fraction and the amount by which the heat release must be decreased thus increases as the square of the diameter. This approximation neglects variations of emissivities etc. with droplet radius, but such effects should be small.

With this modification, the calculation described above can be repeated with radiant energy loss taken into account. From the data shown in Figure 3, however, it seems clear that there is little

point in making such calculations. With very few exceptions, when radiant extinction occurs, it is seen to occur with extinction diameters very close to the initial diameter, in the upper group. For such small diameter changes, the extent of water absorption by the droplet prior to extinction will be very small. There then becomes no point in calculating droplet combustion with water absorption; ordinary droplet-combustion theory will be just as good. It may thus be concluded that, for methanol droplet combustion experiencing radiant extinction, absorption of water (produced by the flame) in the liquid fuel during combustion can be neglected.

It is also noteworthy to observe for the upper group in Figure 3 that the extinction diameters are so close to the initial diameters that the entire combustion process is likely to have been transient, and the extinction diameter is likely to depend on the amount of ignition energy that was provided. In a sense, then, one might wish to consider these atmospheric conditions to lie outside the LOI. The amount of combustion that can be forced to occur is likely proportional to the initiation impulse, the amount of ignition energy provided. Only around the critical transition diameters in 15 % and 16 %  $O_2$  would there be any reason to include radiant energy loss along with water absorption in the liquid.

## Concluding Remarks

Experimental results for methanol droplets of initial diameters in the range 2 to 4 mm burning in oxygen/nitrogen/carbon dioxide atmospheres in microgravity are presented. Measured burning rates, flame standoff ratios and extinction diameters agree reasonably well with simplified theoretical models. For oxygen concentration approximately below 14% radiative extinction was found to occur rather than extinction caused by water absorption. More detailed analyses of these results are currently underway.

## Acknowledgments

This work was funded by NASA ISS Research Program and John M. Hickman served as the project manager. The authors acknowledge the support of ISS crew, and the ground personnel from NASA and Zin Technologies, Inc. in conducting the experiments.

## References

- [1] Daniel L. Dietrich et al. Detailed results from the flame extinguishment experiment (FLEX). Technical Publication NASA/TP-2011-xxxx, NASA, Glenn Research Center, Cleveland OH 44135, USA, December 2011.
- [2] Vedha Nayagam. Quasi-steady flame standoff ratios during methanol droplet combustion in microgravity. *o o e*, 157(1):204–205, 2010.
- [3] B.L. Zhang, J.M. Card, and F.A. Williams. The effect of liquid mass transport on the combustion and extinction of bicomponent droplets of methanol and water. *o o e*, 105:267–290, 1996.
- [4] B.L. Zhang and F.A. Williams. Effects of the Lewis number of water vapor on the combustion and extinction of methanol drops. *o o e*, 112:113–120, 1998.